Effect of Process Parameters on the Electropolymerization Potential and Rate of Formation of Polypyrrole on Stainless Steel

JUDE O. IROH, WENCHENG SU

Department of Materials Science and Engineering, University of Cincinnati, Cincinnati, Ohio 45221-0012

Received 3 December 1996; accepted 31 January 1997

ABSTRACT: Polypyrrole coatings were formed on stainless steel working electrodes in aqueous oxalic acid solution. The rate of formation of polypyrrole coatings on stainless steel increased proportionately with the current density but increased slightly with increased pyrrole concentration. Increasing oxalic acid concentration also had no significant change in the polymerization rate. The electropolymerization potential of pyrrole decreased significantly from 1.5 to 0.8 V versus SCE when the working electrode was polished. The polymerization potential, E_p, of pyrrole, increased however, with increased current density and decreased exponentially with the initial monomer and electrolyte concentration, respectively. © 1997 John Wiley & Sons, Inc. J Appl Polym Sci **66:** 2433–2440, 1997

Key words: polypyrrole; process parameters; electropolymerization potential; electropolymerization rate; stainless steel

INTRODUCTION

Electropolymerization is used in a variety of applications, including the formation of polymers in solution,[1,2] the modification of graphite fibers,[3–6] and the formation of *in situ* matrix composites.[7–10] It is presently being proposed as a technique for forming new materials and novel microstructures.[11] The formation of insulating and highly crosslinked polymer coatings on steel by partial electropolymerization of *o*-allyl phenol and allyl amine on steel was reported.[13] Their coatings showed very good corrosion resistance. One of the approaches to protect steel against oxidation and corrosion is the application of polymeric coatings that are capable of inhibiting the oxidation of steel. Polymer coatings derived from allyl aromatic amines were shown to be very effective inhibitors for the oxidation of iron.[14] Highly stable and corrosion-resistant amine–sulfur copolymer coatings have been formed on steel by electrocopolymerization of aniline and ammonium sulfide.[15] Both insulating and conductive polymer coatings have been electropolymerized onto a variety of substrates[16–20] with excellent throwing power (uniform coating of irregular and complex shapes).

Corrosion takes place when two or more electrochemical reactions [eqs. (1) and (2)] occur on a metal surface, as follows.

$$O_2 + 2H_2O + 4e^- \rightarrow 4OH^- \ (0.4\ V) \qquad (1)$$

(reduction of oxygen)

$$M \rightarrow M^{n+} + ne^- \qquad (2)$$

(oxidation of metal)

Corrosion can be predicted from the following equation

$$\ln K = \frac{nFE_o}{RT} \qquad (3)$$

Correspondence to: J. O. Iroh.

Journal of Applied Polymer Science, Vol. 66, 2433–2440, 1997
 CCC 0021-8995/97/132438-08

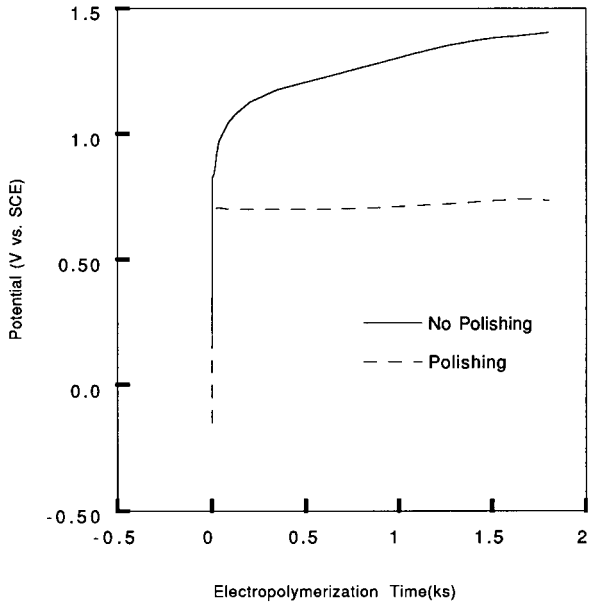

Figure 1 Potential–time curves for electropolymerization of pyrrole onto nonpolished (top) and polished (bottom) stainless steel (Cd = 2.25 mA cm^{-2}).

where n is the number of electrons, F is the Faraday's constant, E_o is the standard cell potential, and K is the equilibrium constant.

The equilibrium potential E is related to the standard potential E_o by the Nernst equation:

$$E = E_o + \frac{RT}{n\mathrm{F}} \ln[\mathrm{M}^{n+}] \qquad (4)$$

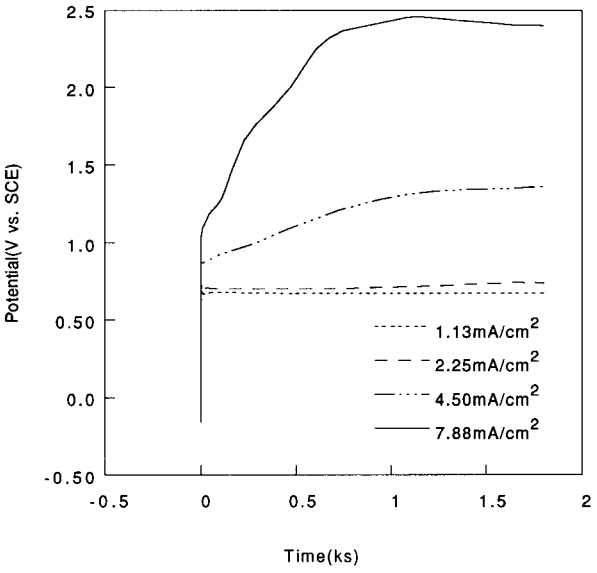

Figure 2 Potential–time curve for electropolymerization of pyrrole onto stainless steel as a function of current density and time, showing no induction time.

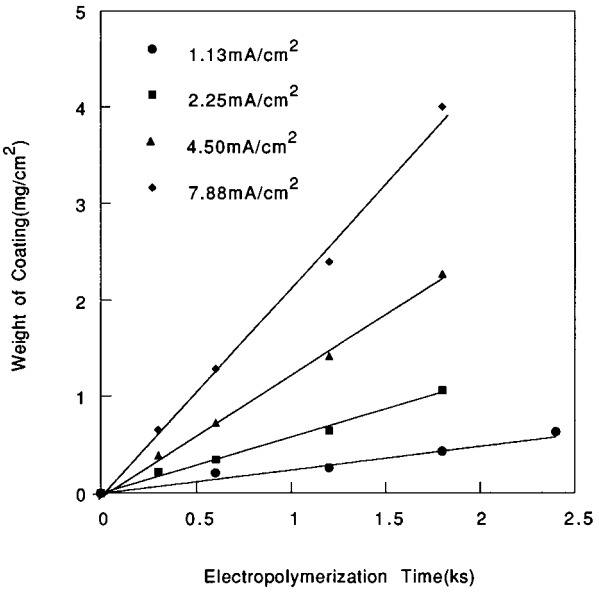

Figure 3 Dependence of the weight of polypyrrole formed onto stainless steel on the current density.

Prevention of corrosion can be achieved by applying passive nonsoluble film on the substrate, minimizing the entry of oxygen and water to the metal–film interface and keeping the oxidation power of the metal as low as possible.[21] The corrosion resistance of stainless steel in formic acid and oxalic acid solutions was investigated by Sekine and Momoi.[22,23] They showed that the room temperature corrosion resistance of stainless steel SUS 329J1 and SS 41 was very good. However, the corrosion resistance of these materials in boiling formic or oxalic acid was poor and decreased with increased acid concentration.[22,23] The formation of free-standing polypyrrole films on stainless steel is of interest because of the low cost of the substrate relative to the conventional platinum electrodes. Judiciously choosing the process variables, strongly adherent polypyrrole films can be formed on stainless steel. The corrosion performance of such coated substrates can be compared with the control. The need for a low-cost and an environmentally friendly metal protection technique has stirred renewed interest in research in this field.

Several investigators have studied the kinetics of electropolymerization of pyrrole on platinum.[24–28] Saveant et al. reported that radical cations coupling, rather than neutral radicals coupling, occurred during the electropolymerization of pyrrole.[24] The dependence of the rate of potentiostatic polymerization of pyrrole on the reaction variables, such as initial pyrrole concentration

Table I Variation of the Rate of Electropolymerization of Pyrrole with Current Density

Applied Current (mA)	Current Density (mA/cm^2)	Electropolymerization Potential (V versus SCE)	Electropolymerization rate ($mg\ cm^{-2}\ ks^{-1}$)
10	1.13	0.67	0.25
20	2.25	0.72	0.59
40	4.50	1.35	1.24
70	7.88	2.40	2.18

and electrolyte concentration, was determined by Otero and coworkers.[25,26] The dependence of the rate of formation of polypyrrole (on platinum electrode) on perchlorate (electrolyte) concentration and pyrrole concentration was found to be 0.5, respectively, in acetonitrile. However, the order of the reaction with respect to perchlorate increased to 0.8 in water. Iroh and Wood also studied the efficiency and kinetics of aqueous potentiostatic electropolymerization of pyrrole on carbon fibers.[27,28] It was shown that the rate of electropolymerization of pyrrole increased with pyrrole concentration, toluene sulfonate concentration and applied voltage raised to a power of 0.8–1.0, 0.8, and 0.9–1.2, respectively,[27] i.e., $R_p\ \alpha\ [M]^{0.8-1.0}\ [SO_3Ph]^{0.8}$, and $[EPa]^{0.9-1.2}$. They showed that the efficiency of potentiostatic polymerization of pyrrole increased with pyrrole concentration and decreased with applied voltage.[28]

In this article, we report the effect of electrochemical process variables on the electropolymerization potential and the rate of formation of polypyrrole on stainless steel. In a future article, the corrosion resistance of the polypyrrole-coated stainless steel will be evaluated and compared with that of polypyrrole-modified low-carbon steel.

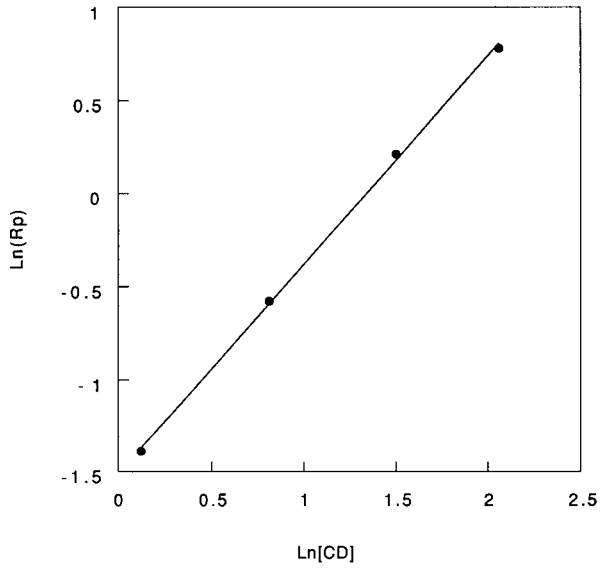

Figure 4 Determination of the current density exponent.

EXPERIMENTAL

Pyrrole (98%) and reagent-grade oxalic acid were purchased from Aldrich Chemical Company, Inc. Tetrachloroethylene and methanol were also purchased from Aldrich Chemical Company. The reagents were dissolved in deionized water prepared in our department.

The working electrode is an 0.46 mm thick 304

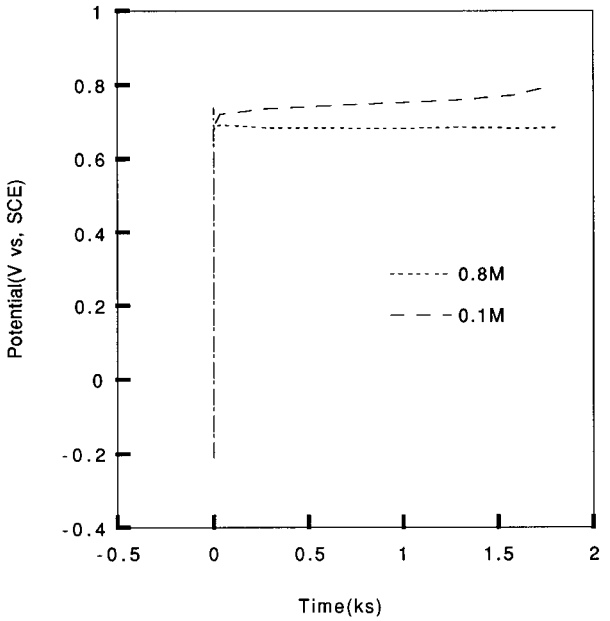

Figure 5 Potential–time curve for electropolymerization of pyrrole onto stainless steel as a function of initial pyrrole concentration and time, showing no induction time.

Table II Variation of the Rate of Electropolymerization of Pyrrole with Pyrrole Concentration

[PY] (*M*)	[OA] (*M*)	Electropolymerization Potential (V versus SCE)	Electropolymerization Rate (mg cm^{-2} ks^{-1})
0.1	0.1	0.76	0.51
0.25	0.1	0.72	0.57
0.5	0.1	0.71	0.69
0.8	0.1	0.68	0.70

stainless steel panel (2B finish) purchased from Copper Brass Sales Inc. The working electrode was degreased with tetrachloroethylene for about 60 min prior to electrochemical polymerization. The counter electrodes comprised of two titanium alloy plates. Saturated Calomel elelectrode (SCE), manufactured by Corning Company, was used as reference electrode. Galvanostatic electropolymerization of pyrrole was performed by an EG&G Princeton Applied Research Potentiostat/ Galvanostat Model 273A.

Electrochemical formation of polypyrrole on stainless steel was carried out in a one-compartment polypropylene cell. The current densities used in this study ranged from 1.13 to 7.88 mA cm^{-2}. The initial electrolyte concentration was varied from 0.05 to 0.4*M,* while pyrrole concentration was varied from 0.1 to 0.8*M.* Electropolymerization time was varied between 300 and 1800 s.

The coated substrate was rinsed with methanol and dried at 65°C in a vacuum oven to constant weight. The weight of the coatings was determined as the difference between the coated and noncoated steel (control).

The infrared (IR) specimens were prepared by mixing a small quantity of the coatings with IR-grade potassium bromide (KBr) powder and subsequent pressing of the mixture into a clear pellet. Transmission IR spectroscopy was carried out using a Bio-Rad FTS-40 spectrophotometer. Elemental analysis of the coatings extracted from coated steel was performed by the Galbraith Laboratories, Inc., Knoxville, Tennessee.

RESULTS AND DISCUSSION

Effect of Current Density

The concentration of pyrrole and oxalic acid were maintained constant at 0.25 and 0.1*M,* respec-

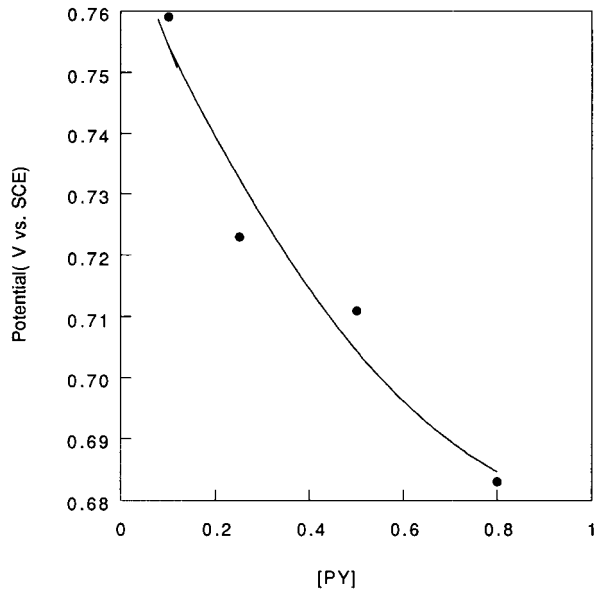

Figure 6 Variation of electropolymerization potential with initial pyrrole concentration.

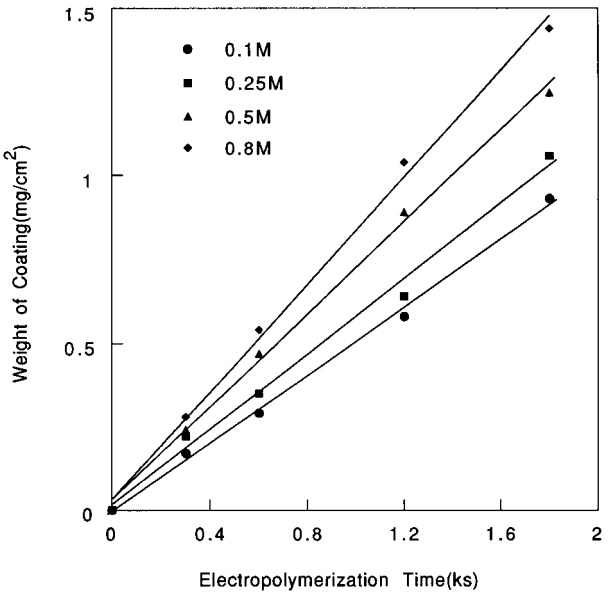

Figure 7 Dependence of the weight of polypyrrole formed onto stainless steel on pyrrole concentration.

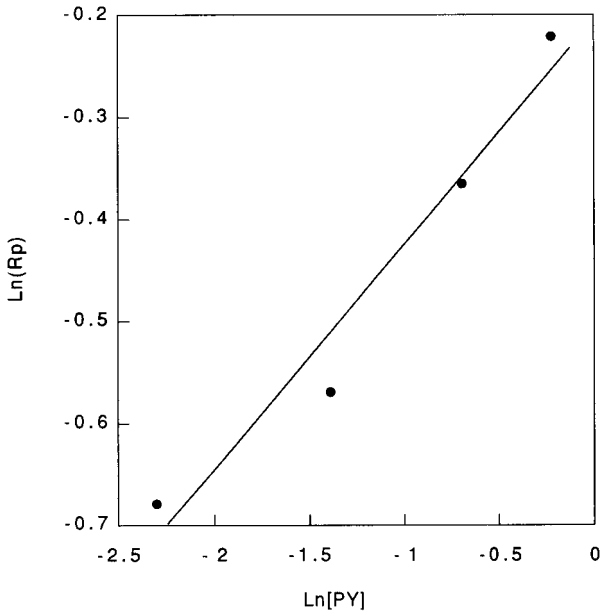

Figure 8 Determination of monomer concentration exponent.

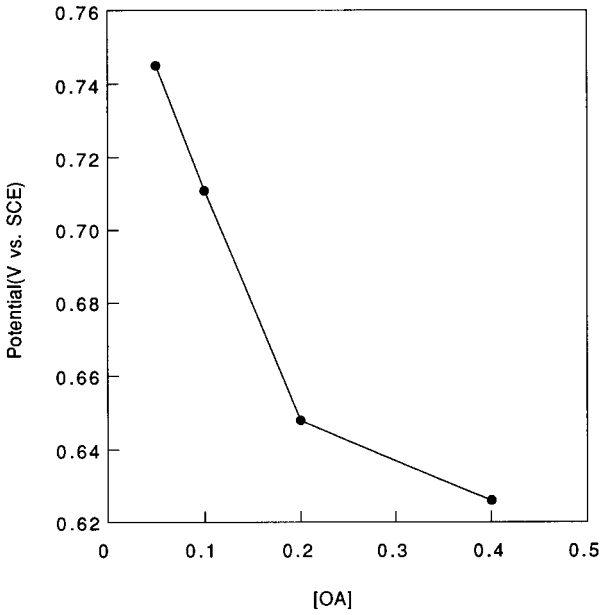

Figure 10 Variation of electropolymerization potential with electrolyte concentration.

tively, and the current density was varied from 1.13 to 7.88 mA cm^{-2}.

Figure 1 shows the dependence of the potential–time curves of pyrrole on stainless steel at 2.25 mA cm^{-2}, on the surface treatment of the substrate. When the stainless steel was polished with abrasive paper, the electropolymerization potential of pyrrole was maintained constant at $E_p \leq 0.8$ V. However, when the stainless steel was not polished, the electropolymerization potential of pyrrole became unsteady and increased sharply to $E_p = 1.5$ V.

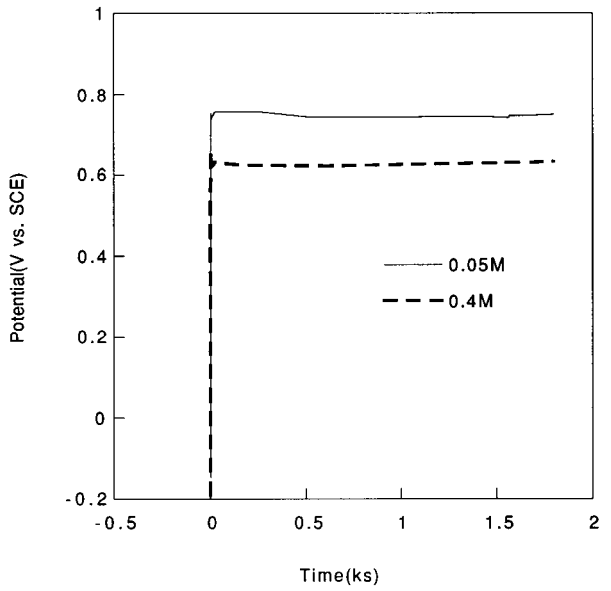

Figure 9 Potential–time curve for electropolymerization of pyrrole onto stainless steel as a function of electrolyte concentration and time, showing no induction time.

The electropolymerization potential of pyrrole increased with the current density, and the shape of the potential–time curves varied with the current density (Fig. 2). Below 2.25 mA cm^{-2}, the electropolymerization potential of pyrrole remained steady at 0.8 V versus SCE during polymerization. Significant increase in the electropolymerization potential of pyrrole to 1.5 V versus SCE occurred when the current density was raised to 4.50 mA cm^{-2}. The electropolymerization potential increased with time and attained a value of 1.35 V versus SCE in 1200 s. A further increase in the current density to 7.88 mA cm^{-2} resulted in a time-dependent increase in the electropolymerization potential for 700 s, after which it remained at 2.40 V versus SCE (Fig. 2).

Figure 3 shows the dependence of the weight of polypyrrole coatings on the current density and electropolymerization time. The weight of the coatings increased proportionately with current density and time. The rate of electropolymerization of pyrrole was determined from the slope of the weight of coating–time curves (Fig. 3). The rate of electropolymerization increased with the current density, as shown in Table I. Increasing the current density from 0.56 to 7.78 mA cm^{-2} resulted in an increase in the rate of polymeriza-

Table III Variation of the Rate of Electropolymerization of Pyrrole with Electrolyte Concentration

[PY] (*M*)	[OA] (*M*)	Electropolymerization Potential (V Versus SCE)	Electropolymerization Rate (mg cm^{-2} ks^{-1})
0.5	0.05	0.74	0.70
0.5	0.1	0.71	0.69
0.5	0.2	0.65	0.67
0.5	0.4	0.63	0.70

tion from 0.25 to 2.18 mg cm^{-2} ks^{-1}. The dependence of the rate of formation of polypyrrole on stainless steel on the current density was determined from the Ln rate versus Ln Cd plot (Fig. 4) to be 1.12 [Rp α $[Cd]^{1.12}$], indicating a first-order process.

Effect of Monomer Concentration

The concentration of oxalic acid and current density were kept constant at 0.1*M* and 2.25 mA cm^{-2}, respectively, while the concentration of pyrrole was varied from 0.1 to 0.8*M*. Figure 5 shows the electropolymerization potential–time curve as a function of initial pyrrole concentration and time. The potential–time curve rose to a maximum value at $t \sim 0$ s, after which it remains invariant with time. There was no induction period, indicating that the chromium oxide layer was effective in preventing the dissolution of iron. The electropolymerization potentials decreased exponentially (about 11% decrease; Table II) with the increased pyrrole concentration (700% increase; Fig. 6) due to increased conductivity of the PPy–C_2O_4 film. Recall that increased current density caused a proportionate increase in the polymerization potential and weight of polypyrrole coatings. The dependence of the weight of polypyrrole on the initial pyrrole concentration is shown on Figure 7. Increasing the pyrrole concentration results in a moderate increase in the weight of polypyrrole formed. For instance, increasing the pyrrole concentration from 0.1 to 0.8*M* (700% increase) resulted in an increase in the weight of coatings from 2.6 to 4.8 mg (85% increase) after 10 min of electropolymerization. The rate of polymerization was determined from the slope of the weight of coatings versus time curve and presented as a function of pyrrole concentration (Table II). The rate of electropolymerization of pyrrole increased with pyrrole concentration (Table II). The order of the electropolymerization with respect to pyrrole concentration was determined from the slope of the Ln rate of weight gain versus Ln [M] plot (Fig. 8) as 0.22 [Rp α $[PY]^{0.22}$].

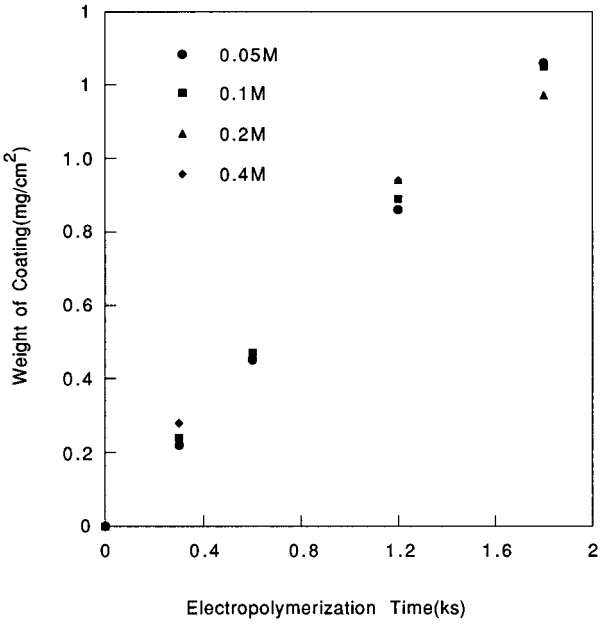

Figure 11 Dependence of the weight of polypyrrole formed onto stainless steel on oxalic acid concentration.

Effect of Electrolyte Concentration

The pyrrole concentration and current density were kept constant at 0.5*M* and 2.25 mA cm^{-2},

Table IV Elemental Composition of the Polypyrrole Coatings

Elements	Composition (%)
C	60.21
H	3.16
N	16.71
S	16.08

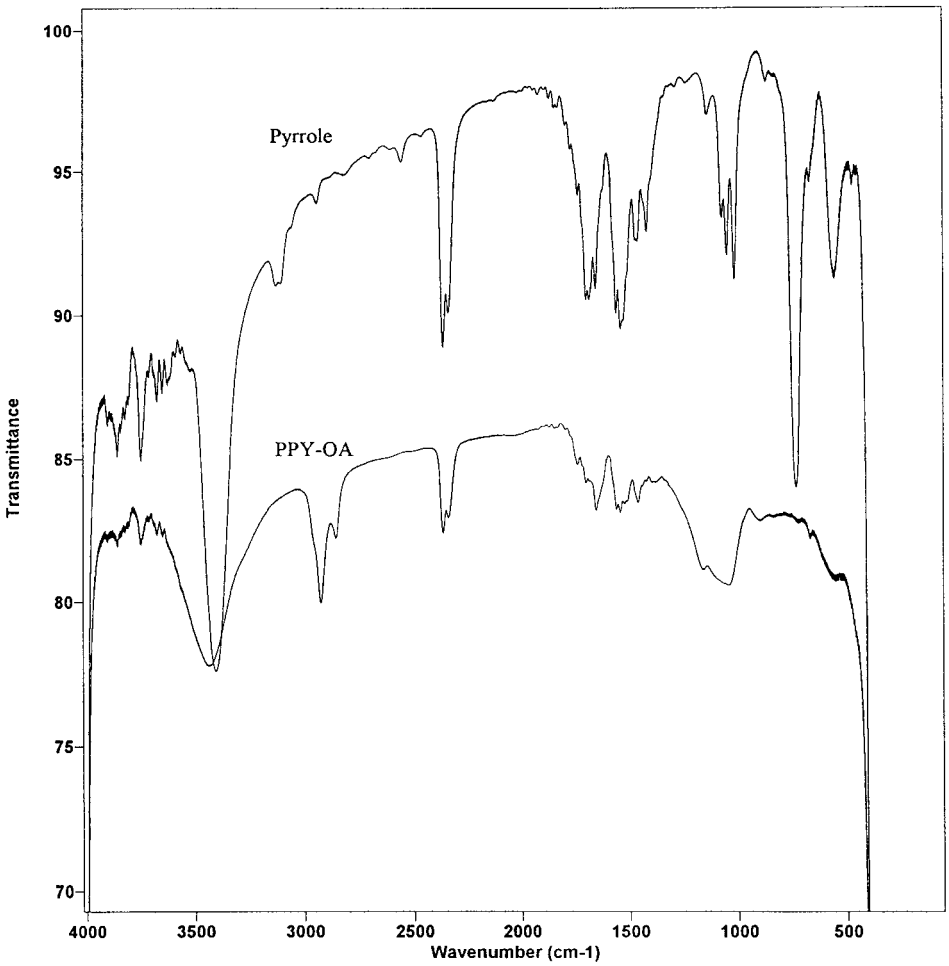

Figure 12 Infrared spectra of pyrrole (top) and polypyrrole–oxalate coatings formed on stainless steel (bottom).

respectively. The concentration of oxalic acid was varied from 0.05 to 0.4*M*. Figures 9 and 10 shows the potential–time curve for electropolymerization of pyrrole as a function of oxalic acid concentration. There was no induction time for polymerization of pyrrole onto stainless steel (Fig. 9). The steady-state polymerization potential decreased (15% decrease) with electrolyte concentration (700% increase; Table III) due to increased conductivity of the PPy-C_2O_4 layer. Generally, the electropolymerization potential decreases exponentially with the increasing electrolyte concentration (Fig. 10). The variation of the weight of polypyrrole coatings with electrolyte concentration is shown in Figure 11. The amount of polypyrrole formed per unit of time is about 0.7 mg cm^{-2} ks^{-1}, irrespective of the oxalic acid concentration (Table III), indicating a zero-order reaction with respect to the electrolyte concentration ($Rp\alpha[OA]_0$).

Elemental Composition and Analysis of the Coatings

The elemental composition of the polypyrrole oxalate coatings formed on stainless steel is shown in Table IV. Elemental analysis shows the presence of oxygen in the coatings and indicates that the hydrogen oxalate counterion is incorporated into the polypyrrole film. The mole ratio of pyrrole to the hydrogen oxalate ion in the film was determined to be $\sim 5 : 1$.

Fourier transform IR (FTIR) spectra of the polypyrrole coatings extracted from stainless steel show the characteristic IR peaks associated with pyrrole and the oxalate counterion. Figure 12 shows the IR spectra for pyrrole (Fig. 12, top) and that for polypyrrole coatings formed in oxalic acid solution (Fig. 12, bottom). The broad peak occurring at 3200–3500 cm^{-1} corresponds to the

N—H stretching in the pyrrole ring. The strong transmittance peak at 2923 cm^{-1} is due to the vibration of the —C—C— group from oxalic acid. The IR peaks occurring between 1650 and 1735 cm^{-1} correspond to C—C stretches, C—H deformations, C—N stretches, N—H deformation, and C=C and C=O stretches. Three distinct bands appear near 1100–1000 cm^{-1} and are due to C—H deformations. The remaining region, 1000–400 cm^{-1}, is dominated by a strong peak near 735 cm^{-1}, (Fig. 12, top), which is due to a C—H wag vibrations coming from adjacent 2,5-hydrogen atoms on the pyrrole ring. There is also a peak near 556 cm^{-1} that probably corresponds to an N—H wag vibration. The remaining peaks in this region can be assigned vibrations, such as other C—H wags, and a couple of different ring vibrations. The IR spectra of the polypyrrole coatings (Fig. 12, bottom) confirmed the presence of the oxalate ion in the coatings (2923, 1650, and 1735 cm^{-1}). One of the striking features of Figure 12 (bottom) is the disappearance of the C—H peak at 735 cm^{-1} due to oxidative coupling (anodic polymerization) of pyrrole. Overall, the IR analysis shows the presence of oxalate ions in the coatings and confirmed the elimination of the 2,5-hydrogen atoms during electropolymerization.

CONCLUSION

Polypyrrole coatings have been successfully formed on stainless steel by aqueous electrochemical polymerization using oxalic acid as the electrolyte. The rate of formation of polypyrrole increased with current density and slightly with initial pyrrole concentration but remained unchanged with electrolyte concentration. The polymerization potential increased with current density and decreased with monomer and electrolyte concentration. The polymerization potential for pyrrole in oxalic acid solution was dependent on the pretreatment of the stainless steel electrode and decreased significantly with surface polish, followed by rinse in tetrachloro ethylene. Overall, smooth and dense polypyrrole films were formed on polished substrates. IR spectra confirmed the presence of oxalate ions in the coatings and the elimination of 2,5-hydrogens during the electropolymerization of pyrrole.

Financial support from the Office of Naval Research's Young Investigators Program, Grant N00014-95-1-0485, is gratefully acknowledged.

REFERENCES

1. B. L. Funt and S. N. Bhdani, *Can. J. Chem.,* **42,** 2733 (1964).
2. B. L. Funt and O. G. Gray, *J. Macromol. Chem.,* **1,** 625 (1966).
3. J. Chang and J. P. Bell, *SAMPE Q.,* **18,** 39 (1987).
4. J. P. Bell, J. Chang, H. W. Rhee, and R. Joseph, *Polym. Comp.,* **8,** 46 (1987).
5. R. V. Subramanian and J. J. Jakubowoskii, *Polym. Eng. Sci.,* **18,** 590 (1978).
6. R. V. Subramanian and J. J. Jakubowoskii, *Org. Coat. Plast. Chem.,* **40,** 688 (1979).
7. J. O. Iroh, J. P. Bell, and D. A. Scola, *J. Appl. Polym. Sci.,* **41,** 735 (1990).
8. J. O. Iroh, J. P. Bell, and D. A. Scola, *Chem. Mater.,* **5,** 78 (1993).
9. J. O. Iroh, Y. Suhng, and M. M. Labes, *J. Appl. Polym. Sci.,* **52,** 1203 (1994).
10. J. O. Iroh, J. P. Bell, D. A. Scola, and J. P. Wesson, *Polym. J.,* **35,** 1306 (1994).
11. P. C. Searson and T. P. Moffat, in *Critical Reviews in Surface Chemistry,* P. Sherwood, Ed., Vol. 3, 1994, pp. 171–238.
12. L. E. A. Berlouis and D. J. Schiffrin, *Trans. IMF,* **64,** 42 (1986).
13. G. Mengoli, P. Bianco, S. Daolio, and M. T. Munari, *J. Electrochem. Soc.,* **128,** 2276 (1981).
14. G. Mengoli, S. Daolio, and M. M. Musiani, *J. Appl. Electrochem.,* **10,** 459, (1981).
15. G. Mengoli, S. Daolio, M. M. Musiani, B. Pelli, and E. Vecchi, *J. Appl. Polym. Sci.,* **28,** 1125 (1983).
16. B. Grunden and J. O. Iroh, *Polym. J.,* **34,** 559 (1995).
17. A. F. Diaz and J. A. Logan, *J. Electroanal. Chem.,* **111,** 111 (1980).
18. M. C. Pham, J. E. Dubois, and P. C. Lacaze, *J. Electroanal. Chem.,* **99,** 331 (1979).
19. F. Bruno, M. C. Pham, and J. E. Dubois, *Electrochim. Acta,* **22,** 451 (1977).
20. G. Mengoli, P. Bianco, S. Daolio, and M. T. Munari, *J. Electrochem. Soc.,* **128,** 2276 (1981).
21. K. B. Tator, in *Metals Handbook,* 9th ed., Vol. 13, L. J. Korb et al., Eds., 1987, pp. 399–418.
22. I. Sekine and K. Momoi, *Corrosion, NACE,* **44,** 136 (1988).
23. I. Sekine and K. Momoi, *Corrosion,* **45,** 924 (1989).
24. J. M. Saveant, *J. Phys. Chem.,* **95,** 10158 (1991).
25. T. F. Otero, J. Rodriguez, E. Angulo, and C. Santamaria, *Synth. Metals,* **41,** 2831 (1991).
26. T. F. Otero and E. Angulo, *J. Appl. Electrochem.,* **22,** 369 (1992).
27. G. A. Wood and J. O. Iroh, *Eur. Polym. J.,* **33,** 107–114 (1997).
28. G. A. Wood and J. O. Iroh, *Synth. Metals,* **80,** 73 (1996).